# Far Infrared Spectrum, *ab Initio* Calculations, and Conformational Analysis of 1-Pentyne

**Stephen Bell,† Gamil A. Guirgis,‡ Yin Li, and James R. Durig***

*Department of Chemistry, University of Missouri−Kansas City, Kansas City, Missouri 64110*

*Received: January 9, 1997; In Final Form: June 2, 1997*[⊗]

The far infrared spectrum of 1-pentyne, $CH_3CH_2CH_2C{\equiv}CH$, has been recorded in the gas phase. The fundamental asymmetric torsional transitions have been observed at 114 and 109 $cm^{-1}$ for the *gauche* (*synclinal*) and *trans* (*antiperiplanar*; methyl group *trans* to the acetylenic group) conformers, respectively. The methyl torsional fundamental (249.8 $cm^{-1}$) has only been observed for the *gauche* conformer. Infrared spectra (3500−400 $cm^{-1}$) of 1-pentyne dissolved in liquid xenon have been recorded from which variable temperature (−60 to −100 °C) studies have been carried out. From these data, the enthalpy difference has been determined to be 113 ± 26 $cm^{-1}$ (323 ± 74 cal/mol) with the *trans* conformer more stable than the *gauche* form. The Raman spectrum (3500−40 $cm^{-1}$) has also been recorded of the liquid to aid in the assignment of the fundamentals. *Ab initio* electronic structure calculations of energies, conformational geometries, vibrational frequencies, and potential energy functions have been carried out to complement and assist in the interpretation of the spectra. In particular, the transitions among torsional energy levels for both the symmetric (methyl) and asymmetric (ethyl) motions have been calculated. The results are compared to the corresponding quantities for some similar molecules.

## Introduction

An analysis of the infrared, Raman, and far infrared spectra of 1,2-pentadiene (ethyl allene) has been recently reported,[1] and assignments of vibrational and torsional frequencies have been made. The 1-pentyne molecule, $HC{\equiv}CCH_2CH_2CH_3$, is a structural isomer of 1,2-pentadiene and is particularly similar in that both have approximately linear C−C−C chains with an attached ethyl group. Additionally, both of these molecules exhibit torsional isomerism in which there are two conformations of approximately the same energy. However, in 1,2-pentadiene the conformers are *synplanar* (called *cis*) and *anticlinal* (called *gauche*) with torsional angles of 0° and approximately 120°, respectively, whereas in 1-pentyne the conformers are *antiperiplanar* (called *trans*) and *synclinal* (called *gauche*) with torsional angles of 180° and 65°, respectively, where 0° is the eclipsed form.

There are more reports of previous spectroscopic studies of 1-pentyne than for 1,2-pentadiene. Two studies of its microwave spectrum have been carried out[2,3] indicating the torsional isomerism mentioned above. Isotopic species were not investigated, so a full geometrical structure has not been obtained from either of these studies.[2,3] The infrared and Raman spectra[4] have, also, been recorded in the gas and liquid phases and assignments made on the basis of normal coordinate calculations. It was necessary to propose two conformers called $C_s$ and $C_1$ to explain the observed bands.[4] The conclusion of a subsequent study[5] of the infrared and Raman spectra of 1-pentyne in the solid phase is that the molecule exists only in the *trans* conformer in the solid. In these studies the low-frequency vibrations including the torsions have been poorly identified or left unassigned, indicating the need for the present study, which includes recording the far infrared spectrum of 1-pentyne in the gas phase.

In one of the microwave studies, the authors[3] concluded that the *gauche* conformer was more stable by 27 ± 36 $cm^{-1}$ (77 ± 103 cal/mol) than the *trans* rotamer. This result differs markedly from that for *n*-butane, where the *trans* conformer is 234 ± 33 $cm^{-1}$ (669 ± 96 cal/mol) more stable than the *gauche* form.[6] Thus, it would be surprising if the acetylenic group could alter the stability by such a large amount. Therefore, in order to determine the conformational stability, we have carried out variable temperature studies of the infrared spectra of 1-pentyne dissolved in liquid xenon.

In conformational studies and vibrational analyses, especially of molecules with one or more internal rotating groups, it has been shown[1] that *ab initio* calculations of potential energy functions and vibrational frequencies have contributed greatly to understanding the molecular dynamics, with the experimental and computational studies both being essential and complementary to each other. For 1-pentyne, it is shown that care must be taken to make calculations at a sufficient level of theory and with an adequate basis set in order to obtain the correct form of the potential energy functions. The results of our vibrational and theoretical study are reported herein.

## Experimental and Computational Methods

The sample of 1-pentyne was purchased from Aldrich Chem. Co, Inc., Milwaukee, WI. Purification was performed with a low-temperature, low-pressure fractionation column. The purity of the sample was checked by recording the mid-infrared spectrum and comparing it to that previously reported[4,5] as well as by mass spectrometry.

The far infrared spectrum of gaseous 1-pentyne, from which the low frequency transitions were obtained, was recorded with a Nicolet Model 200 SXV Fourier transform interferometer equipped with a vacuum bench, a Globar source, a 12.5 $\mu$m Mylar beamsplitter, and a liquid helium-cooled Ge bolometer with a wedged sapphire filter and polyethylene windows. The gas sample was contained in a 1 m cell equipped with polyethylene windows. The spectrum was obtained by recording 256 interferograms at a resolution of 0.1 $cm^{-1}$ which were averaged and transformed with a boxcar truncation function. Typical spectra of low and high pressure are shown in Figure 1.

† Permanent address: Department of Chemistry, University of Dundee, Dundee DD1 4HN, Scotland.

‡ Permanent address: Analytical R & D Department, ICD Division, Bayer Corp., Bushy Park Plant, Charleston, SC 29411.

⊗ Abstract published in *Advance ACS Abstracts,* July 15, 1997.

S1089-5639(97)00163-1 CCC: $14.00 

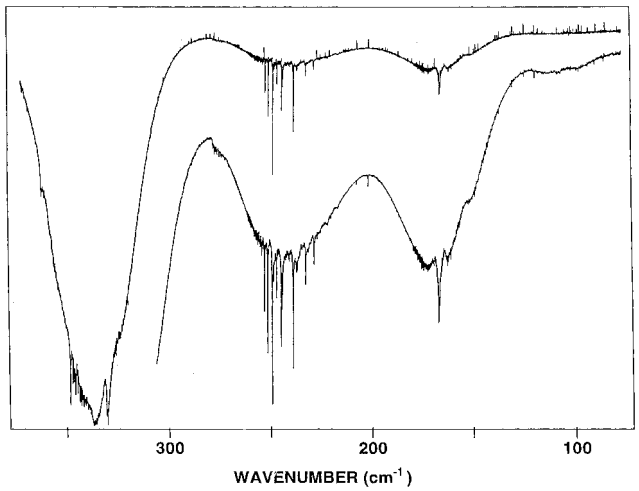


**Figure 1.** Far infrared spectrum of 1-pentyne with upper curve at lower pressure.

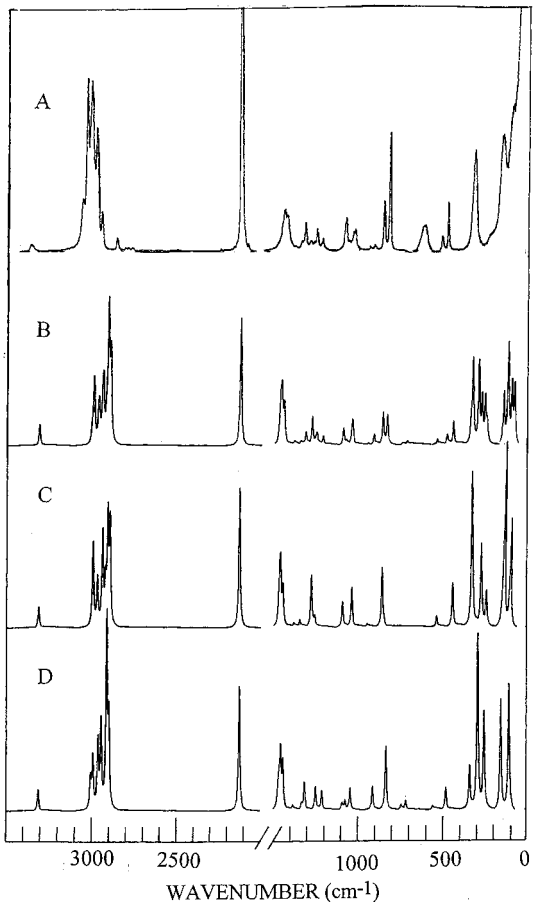


**Figure 2.** Raman spectrum of 1-pentyne: (A) experimental spectrum of the liquid; (B) calculated spectrum of mixture with *trans* conformer more stable with $\Delta H = 113$ cm$^{-1}$; (C) calculated spectrum of pure *gauche* conformer; (D) calculated spectrum of pure *trans* conformer.

The Raman spectrum of the liquid was recorded with a SPEX Model 1400 spectrometer equipped with a Spectra-Physics Model 171 argon ion laser operating on the 5145 Å line with a laser power at the sample of 0.6 W. The sample was sealed in a spherical cell,[7] and a representative spectrum is shown in Figure 2.

The *ab initio* calculations were made with the Gaussian 94 program[8] and the methods employed were Hartree−Fock (HF) and Møller−Plesset (MP) to second order.[9] Full geometric optimization of the structure at energy minima, saddle points, or other specified torsional angles of the methyl and/or ethyl group has been carried out for some of the HF and MP2 energies, and geometrical parameters are reported. Some calculations are single point at optimized geometries from another suitable method, but when energy differences are reported, they have been obtained with a consistent set of optimized geometries. A number of basis sets have been used in order to determine the effect of basis set size and electron correlation on the torsional potential energy functions, in particular on the conformational energy difference of the asymmetric torsional motion.

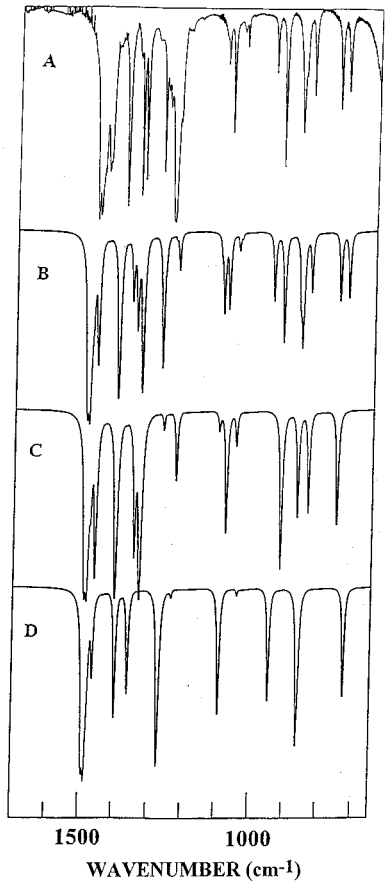


**Figure 3.** Infrared spectrum of 1-pentyne: (A) experimental spectrum of xenon solution; (B) calculated spectrum of mixture with *trans* conformer more stable with $\Delta H = 113$ cm$^{-1}$; (C) calculated spectrum of pure *gauche* conformer; (D) calculated spectrum of pure *trans* conformer.

## Conformational Stability

Variable temperature studies of the infrared spectrum of 1-pentyne dissolved in liquid xenon were conducted to determine the enthalpy difference between the two stable conformers. An important advantage of this temperature study is that the conformer peaks are better resolved and their intensity is more easily measured than bands observed in the infrared spectrum of the gas. Spectral data were obtained at five different temperatures ranging from −100 to −60 °C of the infrared spectrum (Figure 3) from 400 to 3500 cm$^{-1}$. The spectral data for three pairs utilized in the enthalpy determination are listed in Table 1, and typical spectra for the 925/954 conformer pair are shown in Figure 4. The enthalpy difference between the *trans* and *gauche* conformers was calculated by using the van't Hoff equation, $-\ln K = (\Delta H/RT) - \Delta S/R$. A plot of $-\ln K$ versus $1/T$, where $K$ is the ratio of the intensity of a band due to the *trans* conformer to one due to the *gauche* conformer, has a slope that is proportional to the enthalpy difference. The

**TABLE 1: Temperature and Intensity Ratios for Conformer Doublets of 1-Pentyne**

| $T$ (°C) | 1000/$T$ (K) | $I_{925/954}$ | $I_{530/494}$ | $I_{762/494}$ |
|---|---|---|---|---|
| −60 | 4.69 | 4.79 | 1.34 | 0.57 |
| −70 | 4.93 | 4.60 | 1.25 | 0.51 |
| −80 | 5.18 | 4.04 | 1.11 | |
| −100 | 5.78 | 4.10 | 1.12 | 0.46 |
| $\Delta H^a$ | | 101 ± 52 | 111 ± 55 | 127 ± 47 |

[a] Average value is 113 ± 26 cm$^{-1}$ (323 ± 74 cal/mol), with the *trans* form the more stable conformer.

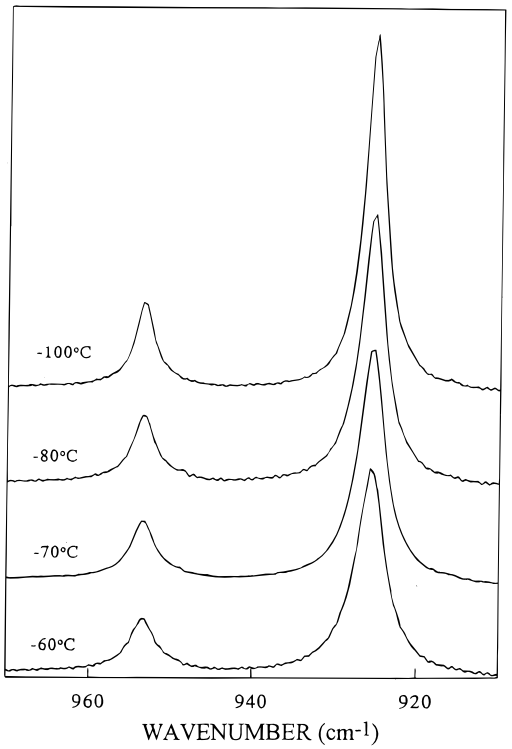


**Figure 4.** Temperature study of the infrared spectrum of the 925/954 cm$^{-1}$ conformer pair of 1-pentyne dissolved in liquid xenon.

*trans* band at 762 cm$^{-1}$ was chosen, but the corresponding mode of the *gauche* rotamer at 730 cm$^{-1}$ is at a frequency where a *trans* fundamental is predicted. Therefore, the *trans* band at 762 cm$^{-1}$ was used with the 494 cm$^{-1}$ band of the *gauche* rotamer to obtain an additional enthalpy value. The data given in Table 1 for the conformer pairs at 925/954, 530/494, and 762/494 cm$^{-1}$ yield values of 101 ± 52 cm$^{-1}$ (289 ± 149 cal/mol) 111 ± 55 (317 ± 157 cal/mol), and 127 ± 47 cm$^{-1}$ (363 ± 134 cal/mol), respectively. The average value for these three determinations is 113 ± 26 cm$^{-1}$ (323 ± 94 cal/mol), with the *trans* rotamer the more stable form. It is expected that this value from the noble gas solution is reasonably close to the value for the vapor since the dipole moments for the *trans* ($\mu$ = 0.853 ± 0.001 D) and *gauche* (0.760 ± 0.006 D) conformers are nearly the same[2] and the volumes for the two conformers are nearly equal.

### *Ab Initio* Calculations

The energies of the *trans* conformation of 1-pentyne obtained by *ab initio* calculations are given in Table 2 for both Hartree−Fock (HF) and Møller−Plesset (MP2) methods and with different basis sets. Full geometry optimization has been carried out for all the different conformations calculated for any particular method and basis set, and where indicated otherwise the geometries have been used in a consistent manner for all conformers. In Table 2, different conformations of 1-pentyne

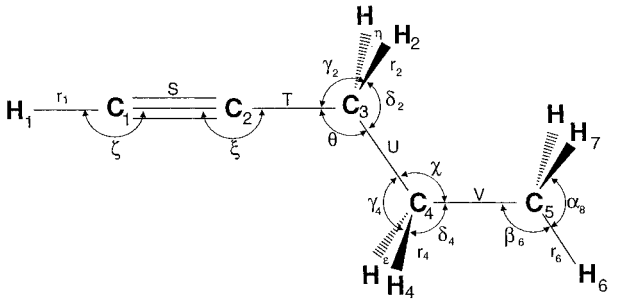


**Figure 5.** Geometric structure and labeling of 1-pentyne.

are labeled with the first symbol in upper case to indicate the ethyl torsion (*trans*, *gauche*, *cis*) and the second symbol in lower case to indicate the methyl torsional angle (staggered or eclipsed). The actual *ab initio* energy is given for the *trans* (Ts) conformer only, and the energies of the other conformers are given relative to the *trans* form. At the Hartree−Fock level the *trans* rotamer is lower in energy than the *gauche* form ($\Delta E$ given in Table 2 as positive) for all basis sets except 3-21G, whereas with the inclusion of electron correlation at the MP2 level the *gauche* conformer is lower in energy than the *trans* form (negative $\Delta E$), but the energy of the *trans* rotamer is always given because of its symmetry and the symmetry of the torsional potential energy function.

It is evident from the data in Table 2 that geometry optimization makes little difference to the conformational energy differences as long as a consistent set of geometrical structures obtained by the same method have been used. It is also evident that the *gauche*−*trans* energy differences obtained with the 6-31G basis set or sets built on it are consistently larger than differences obtained with the DZ basis set or sets built on it. From calculations on similar molecules, it appears that MP2 calculations with DZ plus polarization give potential energy functions more consistent with functions derived from the observed torsional transitions. The lowering of the *gauche* (60°) conformer energy relative to that of the *trans* form on performing MP2 calculations corresponds to increasing the $V_1$ term, i.e. the coefficient of [1 − cos $\tau$], in the potential energy function. This effect is similar to that found in other molecules with ethyl internal tops, such as 1,2-pentadiene[1] and propanal,[10] where the *cis* conformer is lowered in energy relative to the *gauche* rotamer on including electron correlation at the MP2 level.

The geometrical structure parameters of *trans* 1-pentyne obtained by geometry optimizations at the MP2 level are given in Table 3 for only two basis sets, namely, the DZ(d) and 6-31G(d) bases. The labeling of atoms and internal coordinates are given in Figure 5. Although a complete structure of *trans*-1-pentyne has not been obtained from the microwave spectra, accurate rotational constants have been obtained. A structure consistent with these was derived[3] by transfer of parameters from other molecules and by varying the $C_3-C_4$ bond length ($U$) and the $C_2C_3C_4$ and $C_3C_4C_5$ bond angles ($\theta$ and $\chi$). The rotational constants from the structure obtained from MP2 calculations with the 6-31G(d) basis set give better agreement with the observed rotational constants than those obtained from the DZ(d) calculation; this result is again similar to what is observed with related molecules.[1,10] The agreement is surprising in view of the long C≡C bond length obtained at this level, although other parameters are in reasonable agreement. At the HF level, the C≡C bond distance is much too short at 1.189 Å, and it is clear that the 6-31G(d) basis set is not large enough to treat triple bonds adequately.

Geometrical structure parameters for *gauche*-1-pentyne obtained by *ab initio* geometry optimization and from the

**TABLE 2: *Ab Initio* Energies[a] (hartrees) and Energy Differences between Conformers[b] ($cm^{-1}$) for 1-Pentyne**

| | | $\Delta E$ | | | | |
|---|---|---|---|---|---|---|
| | *E* Ts | Gs | Cs | Ss | Te | Ge |
| HF/3-21G | 2.864 221 3 | −52.37 | 1729.35 | 1259.62 | 1062.07 | 1135.57 |
| HF/6-31G | 3.860 682 7 | 53.20 | 1796.87 | 1274.08 | 1028.65 | 1295.87 |
| HF/6-31Gd[c] | 3.931 166 9 | 106.77 | 1881.58 | 1340.12 | 1119.73 | 1134.27 |
| HF/6-31Gdp[c] | 3.944 189 6 | 102.76 | | | | |
| MP2/6-31Gd | 4.573 427 3 | −122.05 | 1619.49 | 1281.21 | 1086.45 | 1176.01 |
| MP2/6-31Gdp[c] | 4.637 253 0 | −118.33 | | | | |
| MP2/6-311+Gdp[c] | 4.744 336 3 | −102.66 | | | | |
| HF/DZ | 3.878 706 5 | 119.48 | 1823.43 | 1241.35 | 1029.20 | 1046.47 |
| HF/DZd[c] | 3.957 023 4 | 169.31 | 1948.07 | 1308.02 | 1109.08 | 1102.92 |
| HF/DZdp[d] | 3.970 707 4 | 156.74 | 1939.42 | 1294.34 | | |
| MP2/DZd[c] | 4.583 736 1 | −73.16 | 1594.43 | 1239.32 | 1031.84 | 1062.67 |
| MP2/DZd | 4.584 103 3 | −74.62 | 1584.77 | 1233.04 | | |
| MP2/DZdp[d] | 4.650 675 8 | −71.89 | 1562.75 | 1212.57 | | |
| MW | | | −31 | 1559 | 1062 | |

[a] Energy of *trans* conformer given as $-(E + 190)$ $E_h$. All MP calculations are frozen core. Geometries fully optimized unless indicated. [b] Conformation labeling: T = *trans*, G = *gauche* ($\tau \approx 60°$), C = *cis*, S = *skew* ($\tau \approx 120°$, barrier between *trans* and *gauche*), s = staggered methyl, and e = eclipsed methyl. $\Delta E$ is given relative to Ts except for Ge, which is relative to Gs. [c] At geometries of MP2/6-31Gd. [d] At geometries of MP2/DZd.

**TABLE 3: Geometrical Parameters[a] for *trans*-1-Pentyne Obtained from *ab Initio* MP2 Calculations and Microwave Spectra**

| | | *trans* | | | *gauche* | | |
|---|---|---|---|---|---|---|---|
| parameter | | MP2 DZ(d) | MP2 6-31G(d) | expt MW[b] | MP2 DZ(d) | MP2 6-31G(d) | expt MW[b] |
| $C_1C_2$ | *S* | 1.229 | 1.221 | 1.210 | 1.229 | 1.221 | 1.210 |
| $C_2C_3$ | *T* | 1.475 | 1.464 | 1.460 | 1.476 | 1.465 | 1.460 |
| $C_3C_4$ | *U* | 1.540 | 1.534 | 1.544 | 1.541 | 1.535 | 1.544 |
| $C_4C_5$ | *V* | 1.533 | 1.525 | 1.536 | 1.533 | 1.525 | 1.536 |
| $C_1C_2C_3$ | $\xi$ | 178.7 | 178.8 | 180.0 | 179.0 | 179.3 | 180.0 |
| $C_2C_3C_4$ | $\theta$ | 112.3 | 112.6 | 111.50 | 112.4 | 112.6 | 111.5 |
| $C_3C_4C_5$ | $\chi$ | 111.6 | 111.9 | 111.50 | 112.6 | 112.7 | 112.4 |
| $C_2C_3C_4C_5$ | $\tau$ | 180.0 | 180.0 | 180.0 | 62.4 | 61.6 | 65.0 |
| $C_1H_1$ | $r_1$ | 1.072 | 1.066 | 1.060 | 1.072 | 1.066 | 1.060 |
| $C_2C_1H_1$ | $\zeta$ | 180.6 | 180.3 | 180.0 | 180.6 | 180.2 | 180.0 |
| $C_3H_2$ | $r_2$ | | | | 1.100 | 1.097 | 1.094 |
| $C_3H_{2,3}$ | $r_{2,3}$ | 1.100 | 1.097 | 1.094 | | | |
| $C_2C_3H_2$ | $\beta_2$ | | | | 108.7 | 109.2 | 109.5 |
| $C_2C_3H_{2,3}$ | $\beta_{2,3}$ | 108.9 | 109.5 | 109.5 | | | |
| $C_3H_3$ | $r_3$ | | | | 1.099 | 1.097 | 1.094 |
| $C_2C_3H_3$ | $\beta_3$ | | | | 108.6 | 109.2 | 109.5 |
| $C_4C_2C_3H_2$[c] | $\phi_2$ | 120.0 | 121.9 | 120.0 | 121.5 | 121.6 | 120.0 |
| $C_4C_2C_3H_3$ | $\phi_3$ | | | | −121.9 | −122.2 | −120.0 |
| $C_4H_4$ | $r_4$ | | | | 1.100 | 1.096 | 1.094 |
| $C_4H_{4,5}$ | $r_{4,5}$ | 1.099 | 1.095 | 1.094 | | | |
| $C_4H_5$ | $r_5$ | | | | 1.099 | 1.095 | 1.094 |
| $C_3C_4H_4$ | $\beta_4$ | | | | 108.0 | 108.2 | 109.5 |
| $C_3C_4H_{4,5}$ | $\beta_{4,5}$ | 108.8 | 108.9 | 109.5 | | | |
| $C_3C_4H_5$ | $\beta_5$ | | | | 108.8 | 108.8 | 109.5 |
| $C_5C_3C_4H_4$[c] | $\phi_4$ | 121.8 | 122.1 | 120.0 | 121.4 | 121.9 | 120.0 |
| $C_5C_3C_4H_5$ | $\phi_5$ | | | | −122.2 | −122.3 | −120.0 |
| $C_5H_6$ | $r_6$ | 1.098 | 1.094 | 1.094 | 1.098 | 1.094 | 1.094 |
| $C_4C_5H_6$ | $\beta_6$ | 110.9 | 111.1 | 110.1 | 110.7 | 111.0 | 110.14 |
| $C_3C_4C_5H_6$ | $\phi_6$ | 180.0 | 180.0 | 180. | 178.6 | 179.3 | 180.0 |
| $C_5H_7$ | $r_7$ | | | | 1.097 | 1.093 | 1.094 |
| $C_4C_5H_7$ | $\beta_7$ | | | | 110.8 | 110.7 | 110.14 |
| $C_3C_4C_5H_7$ | $\phi_7$ | | | | −61.2 | −60.4 | −60.0 |
| $C_5H_{7,8}$ | $r_{7,8}$ | 1.099 | 1.094 | 1.094 | | | |
| $C_4C_5H_{7,8}$ | $\beta_{7,8}$ | 110.9 | 111.0 | 110.1 | | | |
| $C_3C_4C_5H_7$[c] | $\phi_7$ | 60.0 | 60.0 | 60.0 | | | |
| $C_5H_8$ | $r_8$ | | | | 1.099 | 1.095 | 1.094 |
| $C_4C_5H_8$ | $\beta_8$ | | | | 110.7 | 110.8 | 110.14 |
| $C_3C_4C_5H_8$ | $\phi_8$ | | | | 58.8 | 59.4 | 60.0 |
| rotational constants | | | | | | | |
| | *A* | 23205.6 | 23466.6 | 23340.0 | 9778.28 | 9873.16 | 9921.11 |
| | *B* | 2201.33 | 2220.29 | 2230.57 | 3146.40 | 3178.64 | 3172.78 |
| | *C* | 2089.58 | 2107.68 | 2116.39 | 2609.69 | 2633.65 | 2634.03 |
| | $\kappa$ | −0.9894 | −0.9894 | −0.989 | −0.8503 | −0.8494 | −0.852 |
| | $I_\tau$ | 3.1850 | 3.1534 | 3.1896 | 3.1889 | 3.1585 | 3.1896 |
| | *F* | 6.0936 | 6.1553 | 6.0916 | 5.4068 | 5.4583 | 5.4100 |

[a] Bond lengths in angstroms, angles in degrees, rotational constants in MHz, $I_\tau$ in amu Å$^2$, and *F* in $cm^{-1}$. [b] Reference 3. [c] Dihedral angle of symmetrically equivalent H is negative value.

**TABLE 4: Symmetry Coordinates for Vibrations of *trans*-1-Pentyne**

| species | description | coordinate |
|---|---|---|
| A′ | ≡C−H stretch | $S_1 = r_1$ |
| | $CH_3$ antisymmetric stretch | $S_2 = 2r_6 - r_7 - r_8$ |
| | $CH_2$ symmetric stretch | $S_3 = r_4 + r_5$ |
| | $CH_3$ symmetric stretch | $S_4 = r_6 + r_7 + r_8$ |
| | C′$H_2$ symmetric stretch[a] | $S_5 = r_2 + r_3$ |
| | C≡C stretch | $S_6 = S$ |
| | $CH_3$ antisymmetric deformation | $S_7 = 2\alpha_6 - \alpha_7 - \alpha_8$ |
| | $CH_2$ scissors | $S_8 = (\sqrt{6}+2)\epsilon + (\sqrt{6}-2)\chi - \gamma_4 - \gamma_5 - \delta_4 - \delta_5$ |
| | C′$H_2$ scissors | $S_9 = (\sqrt{6}+2)\eta + (\sqrt{6}-2)\theta - \gamma_2 - \gamma_3 - \delta_2 - \delta_3$ |
| | $CH_3$ symmetric deformation | $S_{10} = \alpha_6 + \alpha_7 + \alpha_8 - \beta_6 - \beta_7 - \beta_8$ |
| | $CH_2$ wag | $S_{11} = \gamma_4 + \gamma_5 - \delta_4 - \delta_5$ |
| | C′$H_2$ wag | $S_{12} = \gamma_2 + \gamma_3 - \delta_2 - \delta_3$ |
| | $CH_3$ rock | $S_{13} = 2\beta_6 - \beta_7 - \beta_8$ |
| | C′−C−C antisymmetric stretch | $S_{14} = U - V$ |
| | ≡C−C′ stretch | $S_{15} = T$ |
| | C′−C−C symmetric stretch | $S_{16} = U + V$ |
| | C≡C−H bend | $S_{17} = \zeta$ |
| | C′−C−C bend | $S_{18} = (\sqrt{6}-2)\epsilon - (\sqrt{6}+2)\chi - \gamma_4 - \gamma_5 - \delta_4 - \delta_5$ |
| | C−C′−C bend | $S_{19} = (\sqrt{6}-2)\eta - (\sqrt{6}+2)\theta - \gamma_2 - \gamma_3 - \delta_4 - \delta_5$ |
| | C≡C−C′ bend | $S_{20} = \xi$ |
| | redundancy | $S_{1R} = \chi + \epsilon + \gamma_4 + \gamma_5 + \delta_4 + \delta_5$ |
| | redundancy | $S_{2R} = \theta + \eta + \gamma_2 + \gamma_3 + \delta_2 + \delta_3$ |
| | redundancy | $S_{3R} = \alpha_6 + \alpha_7 + \alpha_8 + \beta_6 + \beta_7 + \beta_8$ |
| A″ | $CH_3$ antisymmetric stretch | $S_{21} = r_7 - r_8$ |
| | $CH_2$ antisymmetric stretch | $S_{22} = r_4 - r_5$ |
| | C′$H_2$ antisymmetric stretch | $S_{23} = r_2 - r_3$ |
| | $CH_3$ antisymmetric deformation | $S_{24} = \alpha_7 - \alpha_8$ |
| | $CH_2$ twist | $S_{25} = \gamma_4 - \gamma_5 - \delta_4 + \delta_5$ |
| | C′$H_2$ twist | $S_{26} = \gamma_2 - \gamma_3 - \delta_2 + \delta_3$ |
| | C′$H_2$ rock | $S_{27} = \gamma_2 - \gamma_3 + \delta_2 - \delta_3$ |
| | $CH_3$ rock | $S_{28} = \beta_7 - \beta_8$ |
| | $CH_2$ rock | $S_{29} = \gamma_4 - \gamma_5 + \delta_4 - \delta_5$ |
| | C≡C−H bend | $S_{30} = \zeta'$ |
| | C≡C−C′ bend | $S_{31} = \xi'$ |
| | $CH_3$ torsion | $S_{32} = \tau_1$ |
| | asymmetric torsion | $S_{33} = \tau_2$ |

[a] Since there are two methylene groups, $C_3$ is marked C′.

microwave data are given in Table 3. The microwave structure is identical to that for the *trans* form in Table 2 except that the torsional angle $\tau$ and the bond angle $\chi$ have been varied to fit the *A* rotational constant. Once again the rotational constants from the 6-31G(d) calculations are in surprisingly good agreement with the observed values; this is especially remarkable, as the torsional angle $\tau$ differs by 3.5°. In propanal[10] and 1-butene,[11] adjusting the torsional angle in the *ab initio gauche* structure to the microwave $r_0$ or $r_s$ values gives excellent agreement of all calculated rotational constants with the microwave values. In 1-pentyne, adjusting the torsional angle $\tau$ toward the microwave value gives better agreement for the *A* constant at $\tau = 63°$ but no better agreement for the *B* and *C* constants, and it appears that in the unadjusted MP2 structure the low value of $\tau$ is compensated by the long bond lengths.

### Vibrational Assignment

The infrared and Raman spectra of 1-pentyne have previously been obtained[4,5] in the gas, liquid, and solid phases. In the present study, vibrational frequencies have been obtained from force constants calculated by *ab initio* methods up to the MP2 level. It is well-known that such *ab initio* force constants require scaling, although less severe scaling is required for MP2 force constants than for those from HF calculations. In order to apply different scale factors to different types of internal coordinates, a full vibrational analysis is needed. The symmetry coordinates used in this study of 1-pentyne are defined in Table 4. There are 23 A′ and 13 A″ coordinates including three redundancies. The $C_3-C_4$ and $C_4-C_5$ stretching coordinates have been combined to give symmetrical and antisymmetrical stretching modes.

The force field in Cartesian coordinates was calculated by the Gaussian 94 program[8] with the MP2/6-31G(d) basis set. The Cartesian coordinates obtained from the optimized geometry were used to calculate the **B** matrix elements with the **G** matrix program of Schachtschneider.[12] The resulting **B** matrix was used to convert the *ab initio* force field in Cartesian coordinates to a force field in internal coordinates. The force fields for the *trans* and *gauche* conformers can be obtained from the authors. Initially, all scaling factors were kept at a value of 1.0 to produce pure *ab initio* calculated vibrational frequencies. Calculated and observed vibrational frequencies of the *trans* and *gauche* conformers are given in Table 5. It can be seen that unscaled HF vibrational frequencies are all much higher than observed, whereas unscaled MP2 frequencies are closer to the experimental values. Because of the inadequacy of the basis set used (6-31G[d]) to describe the C≡C bonds well, more scale factors than usual are employed. The force constants for C−C stretches were scaled by 0.9 except that the C≡C stretch was scaled by 0.98. All the other force constants (C−H stretches and deformations) were scaled by 0.88, except the C−C−C bends (including C≡C−C linear bends) and C≡C−H bends, and torsions were not scaled (factor 1.0). Calculated infrared intensities and Raman activities obtained from MP2 calculations without scaling are listed in Table 5. Although the symmetry labels A′ and A″ do not apply to the *gauche* conformer, the symmetry coordinate definitions and the numbering of frequencies $\nu_1-\nu_{33}$ were retained for the vibrational fundamentals of the *gauche* conformer for easy comparison with the corresponding modes for the *trans* conformer.

There are a few of the fundamentals that must be reassigned from those previously given.[4,5] For example, the C′$H_2$ wag,

**TABLE 5: Vibrational Frequencies ($cm^{-1}$) of *trans* and *gauche* 1-Pentyne**

| | | | *trans* | | | | | | | | *gauche* | | | | | | | |
|---|---|---|---|---|---|---|---|---|---|---|---|---|---|---|---|---|---|---|
| species | vib. no. | description | HF 6-31Gd unscaled | MP2 6-31Gd unscaled | MP2 6-31Gd scaled | IR int.[b] | obs.[a] | Raman act.[b] | DP ratios | P.E.D. | HF 6-31Gd unscaled | MP2 6-31Gd unscaled | MP2 6-31Gd scaled | IR int.[b] | obs.[a] | Raman act.[b] | DP ratios | P.E.D. |
| A′ | $\nu_1$ | ≡C−H stretch | 3664 | 3522 | 3311 | 52.8 | 3329 | 33.0 | 0.22 | $96S_1$ | 3664 | 3522 | 3311 | 51.1 | 3329 | 32.9 | 0.23 | $96S_1$ |
| | $\nu_2$ | $CH_3$ antisymmetric stretch | 3268 | 3195 | 2997 | 25.5 | 2970 | 86.2 | 0.69 | $99S_2$ | 3265 | 3192 | 2994 | 32.2 | 2970 | 65.4 | 0.70 | $63S_2,33S_{21}$ |
| | $\nu_3$ | $CH_2$ symmetric stretch | 3218 | 3116 | 2923 | 24.1 | 2914 | 46.5 | 0.24 | $96S_3$ | 3213 | 3106 | 2914 | 16.1 | 2914 | 24.9 | 0.42 | $64S_3,33S_4$ |
| | $\nu_4$ | $CH_3$ symmetric stretch | 3208 | 3102 | 2910 | 19.7 | 2873 | 129.1 | 0.01 | $99S_4$ | 3205 | 3106 | 2913 | 28.0 | 2880 | 206.5 | 0.06 | $66S_4,32S_3$ |
| | $\nu_5$ | C′$H_2$ symmetric stretch | 3198 | 3089 | 2897 | 11.3 | 2873 | 122.2 | 0.08 | $98S_5$ | 3202 | 3092 | 2900 | 14.3 | 2880 | 101.4 | 0.11 | $98S_5$ |
| | $\nu_6$ | C≡C stretch | 2412 | 2167 | 2128 | 0.19 | 2127 | 104.4 | 0.29 | $83S_6,15S_{15}$ | 2410 | 2164 | 2126 | 0.02 | 2127 | 92.1 | 0.28 | $83S_6,15S_{15}$ |
| | $\nu_7$ | $CH_3$ antisymmetric stretch | 1653 | 1571 | 1474 | 5.6 | 1467 | 3.0 | 0.70 | $51S_7,39S_8$ | 1645 | 1564 | 1467 | 6.5 | 1459 | 11.2 | 0.71 | $75S_7$ |
| | $\nu_8$ | $CH_2$ scissors | 1638 | 1557 | 1461 | 0.8 | 1460 | 22.5 | 0.74 | $54S_8,41S_7$ | 1636 | 1553 | 1458 | 0.9 | 1460 | 24.1 | 0.75 | $80S_8$ |
| | $\nu_9$ | C′$H_2$ scissors | 1627 | 1542 | 1447 | 1.2 | 1435 | 15.8 | 0.74 | $92S_9$ | 1625 | 1539 | 1444 | 3.8 | 1435 | 19.5 | 0.73 | $93S_9$ |
| | $\nu_{10}$ | $CH_3$ symmetric deformation | 1568 | 1472 | 1381 | 2.5 | 1381 | 2.0 | 0.73 | $93S_{10}$ | 1570 | 1474 | 1384 | 6.6 | 1381 | 2.2 | 0.58 | $88S_{10}$ |
| | $\nu_{11}$ | $CH_2$ wag | 1537 | 1433 | 1346 | 1.8 | 1351 | 3.0 | 0.52 | $52S_{11},31S_{12}$ | 1515 | 1418 | 1332 | 2.6 | 1340 | 2.3 | 0.60 | $70S_{11}$ |
| | $\nu_{12}$ | C′$H_2$ wag | 1436 | 1339 | 1259 | 5.4 | 1276 | 3.6 | 0.60 | $57S_{12},27S_{11}$ | 1502 | 1401 | 1316 | 6.9 | 1328 | 10.8 | 0.62 | $60S_{12},25S_{25}$ |
| | $\nu_{13}$ | $CH_3$ rock | 1213 | 1151 | 1095 | 2.4 | 1093 | 7.6 | 0.14 | $39S_{13},24S_{16},12S_{19}$ | 1200 | 1132 | 1075 | 2.0 | 1077 | 2.9 | 0.73 | $32S_{13},15S_{13},15S_{27}$ |
| | $\nu_{14}$ | C′CC antisymmetric stretch | 1119 | 1096 | 1040 | 0.1 | 1040 | 11.4 | 0.64 | $79S_{14}$ | 1136 | 1106 | 1046 | 0.4 | 1048 | 6.3 | 0.70 | $54S_{14},11S_{12},10_{11}$ |
| | $\nu_{15}$ | ≡C−C′ stretch | 1021 | 997 | 949 | 2.0 | 954 | 1.0 | 0.58 | $53S_{15},25S_{16}$ | 999 | 965 | 914 | 3.4 | 925 | 5.8 | 0.73 | $37S_{15},22S_{16},22S_{13}$ |
| | $\nu_{16}$ | C′CC symmetric stretch | 946 | 908 | 862 | 3.5 | 872 | 13.4 | 0.27 | $28S_{16},35S_{13},15S_{15}$ | 907 | 880 | 836 | 1.5 | 840 | 13.7 | 0.13 | $53S_{16},15S_{27},12S_{15}$ |
| | $\nu_{17}$ | C≡C−H level | 801 | 545 | 541 | 45.0 | 633 | 1.4 | 0.18 | $68S_{17},12S_{20}$ | 802 | 566 | 560 | 32.3 | 633 | 0.6 | 0.38 | $46S_{17},19S_{18},15S_{20}$ |
| | $\nu_{18}$ | C′CC bend | 554 | 453 | 447 | 7.4 | 494 | 4.2 | 0.50 | $37S_{18},33S_{17},11S_{16}$ | 589 | 489 | 484 | 19.1 | 530 | 2.4 | 0.75 | $57S_{17},26S_{18},11S_{19}$ |
| | $\nu_{19}$ | CC′C bend | 373 | 335 | 330 | 0.15 | 331[c] | 3.9 | 0.63 | $67S_{19},17S_{20}$ | 375 | 349 | 344 | 0.14 | 337[c] | 2.8 | 0.71 | $58S_{19},10S_{20}$ |
| | $\nu_{20}$ | C≡C−C′ bend | 177 | 139 | 138 | 0.022 | 153[c] | 9.3 | 0.74 | $64S_{20},32S_{18}$ | 191 | 160 | 160 | 0.061 | 168[c] | 7.4 | 0.72 | $54S_{20},25S_{18},11S_{32}$ |
| A″ | $\nu_{21}$ | $CH_3$ antisymmetric stretch | 3271 | 3192 | 2995 | 43.5 | 2970 | 25.3 | 0.75 | $82S_{21}$ | 3282 | 3205 | 3007 | 23.6 | 2970 | 39.1 | 0.72 | $61S_{21},37S_2$ |
| | $\nu_{22}$ | $CH_2$ antisymmetric stretch | 3247 | 3166 | 2970 | 7.8 | 2943 | 59.4 | 0.75 | $74S_{22}$ | 3248 | 3159 | 2964 | 17.7 | 2943 | 83.7 | 0.74 | $85S_{22}$ |
| | $\nu_{23}$ | C′$H_2$ antisymmetric stretch | 3233 | 3133 | 2940 | 5.1 | 2943 | 114.0 | 0.75 | $91S_{23}$ | 3239 | 3140 | 2946 | 14.0 | 2943 | 105.6 | 0.65 | $90S_{23}$ |
| | $\nu_{24}$ | $CH_3$ antisymmetric deformation | 1643 | 1564 | 1467 | 7.7 | 1459 | 19.2 | 0.75 | $93S_{24}$ | 1652 | 1571 | 1474 | 5.9 | 1467 | 5.9 | 0.75 | $79S_{24},13S_8$ |
| | $\nu_{25}$ | $CH_2$ twist | 1447 | 1364 | 1279 | 0.0 | 1282 | 19.2 | 0.75 | $64S_{25},27S_{26}$ | 1416 | 1332 | 1251 | 0.2 | 1240 | 8.5 | 0.58 | $46S_{25},18S_{12},17S_{28}$ |
| | $\nu_{26}$ | C′$H_2$ twist | 1381 | 1302 | 1222 | 0.1 | 1240 | 0.5 | 0.75 | $40S_{26},24S_{28},20S_{29},12S_{25}$ | 1372 | 1291 | 1214 | 0.9 | | 6.8 | 0.56 | $61S_{26}$ |
| | $\nu_{27}$ | C′$H_2$ rock | 1236 | 1159 | 1090 | 0.1 | 1095 | 0.4 | 0.75 | $26S_{27},28S_{26},18S_{29},15S_{28}$ | 1232 | 1159 | 1093 | 0.2 | | 2.2 | 0.49 | $23S_{27},17S_{28},13S_{29},11S_{27}$ |
| | $\nu_{28}$ | $CH_3$ rock | 952 | 903 | 849 | 0.8 | 840 | 0.5 | 0.75 | $36S_{28},39S_{27},16S_{25}$ | 962 | 914 | 745 | 1.6 | 762 | 1.1 | 0.57 | $41S_{28},20S_{28},11S_{13}$ |
| | $\nu_{29}$ | $CH_2$ rock | 801 | 764 | 718 | 1.9 | 740 | 0.1 | 0.75 | $59S_{29},23S_{27},1228$ | 822 | 792 | 718 | 1.8 | 740 | 1.7 | 0.14 | $49S_{29},20S_{28},13S_{15}$ |
| | $\nu_{30}$ | C≡C−H bend | 791 | 517 | 516 | 53.3 | 628 | 0.0 | 0.75 | $98S_{30}$ | 792 | 522 | 521 | 52.9 | 628 | 0.1 | 0.53 | $99S_{30}$ |
| | $\nu_{31}$ | C≡C−C′ bend | 401 | 278 | 278 | 0.047 | 362[c] | 11.4 | 0.75 | $70S_{31},18S_{33}$ | 402 | 298 | 297 | 0.12 | 348[c] | 9.2 | 0.76 | $43S_{31},18S_{32},21S_{33}$ |
| | $\nu_{32}$ | $CH_3$ torsion | 257 | 248 | 248 | 0.0002 | 240[c] | 1.4 | 0.75 | $89S_{32},10S_{31}$ | 281 | 259 | 259 | 0.17 | 250[c] | 4.1 | 0.75 | $66S_{32},30S_{31}$ |
| | $\nu_{33}$ | asymmetric torsion | 108 | 100 | 99 | 0.019 | 106 | 3.0 | 0.75 | $79S_{33},16S_{31}$ | 122 | 115 | 115 | 0.074 | 114[c] | 4.6 | 0.72 | $66S_{33},17S_{31},11S_{20}$ |

[a] From ref 4. [b] Infrared intensities in km $mol^{-1}$; Raman activities in $A^4$/amu. [c] From far infrared in this study.

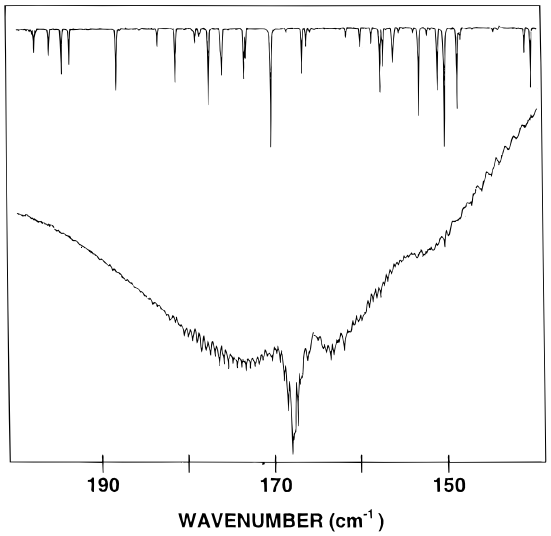


**Figure 6.** $C_3'C_4C_5$ bending mode, $\nu_{20}$, of 1-pentyne. The upper trace is the spectrum of water.

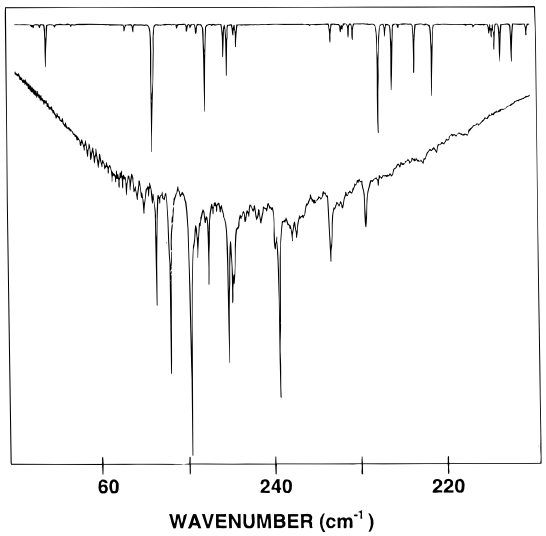


**Figure 7.** Methyl torsional bands of 1-pentyne.

$\nu_{12}$, for the *gauche* conformer is predicted more than 50 $cm^{-1}$ higher than the corresponding mode for the *trans* rotamer, whereas these modes were previously assigned as accidentally degenerate. Therefore, this mode has been assigned to the 1328 $cm^{-1}$ band, which had previously been attributed to the $CH_2$ wag, $\nu_{11}$. The $CH_2$ wag for the *gauche* conformer is now assigned to the band at 1340 $cm^{-1}$, with the corresponding mode for the *trans* conformer assigned at 1351 $cm^{-1}$.

For the lower frequencies, measurements of bands were made from the far infrared spectrum reported in this study. Examples of the spectrum are shown in Figure 1. The skeletal modes $\nu_{19}$, $\nu_{20}$, and $\nu_{31}$ are assigned on the basis of the *ab initio* calculations (scale factor for these modes all 1.0), and the observed frequencies are listed in Table 5 for the *trans* and *gauche* conformers. The strong and broad band around 337 $cm^{-1}$ is assigned to the $C_2-C_3'-C_4$ bending mode $\nu_{19}$. Since a depolarized band is observed at 339 $cm^{-1}$ in the Raman spectrum of 1-pentyne, the main hump at 337 $cm^{-1}$ is assigned to $\nu_{19}$ of the *gauche* conformer. The slightly weaker spike at 331 $cm^{-1}$ is assigned to the same mode of the *trans* conformer. The medium intense but still prominent Q spike at 168.0 $cm^{-1}$ (Figure 6) is assigned to the $C_3'-C_4-C_5$ bending mode $\nu_{20}$ of the *gauche* conformer for three reasons. It is predicted to be 3 times stronger and at a higher frequency than that for the *trans* rotamer, but especially because the rotational fine structure around the central peak must be that of the *gauche* conformer and not the *trans* rotamer. The intervals among the sub-bands are between 0.43 and 0.50 $cm^{-1}$, which corresponds approximately to $2\tilde{A}$ ($2A - [B + C]$) of the *gauche* form. The $\tilde{A}$ values of the *gauche* and *trans* conformers are quite different, with values of 0.23 and 0.71 $cm^{-1}$, respectively. A shoulder, perhaps due to an R branch of a B-type band of a nearly symmetric top, is seen at 153 $cm^{-1}$ with a faint sub-band structure of mean interval 1.12 $cm^{-1}$ and is assigned to the $C_3'-C_4-C_5$ bending mode $\nu_{20}$, of the *trans* conformer.

There are a number of problems with the assignment of the $C\equiv C-C'$ out-of-plane bending mode $\nu_{31}$ of both conformers, as they are both predicted with reasonable intensity where there are no strong bands in the spectrum in the expected region (278 and 297 $cm^{-1}$). However, since the other bending modes associated with the $C\equiv C$ group are predicted at too low frequencies from the MP2/6-31G(d) calculations, $\nu_{31}$ is probably affected in the same way. Using the mean of the HF and MP2 predictions, it is expected that these modes probably fall near the strong feature around 340 $cm^{-1}$ and are swamped by the stronger $C-C-C$ bending bands. The sharp peak at 348 $cm^{-1}$ appearing near the top of the $\nu_{19}$ peak (Figure 1) and the weaker shoulder at 362 $cm^{-1}$ may therefore be assigned to $\nu_{31}$ for the *gauche* and *trans* conformers, respectively, or vice versa.

For frequencies above 400 $cm^{-1}$ for both conformers, the agreement between observed[4,5] and calculated (scaled) frequencies is relatively good, except for the modes involving the $C\equiv C$ group. In particular, $\nu_{17}$ and $\nu_{30}$, the in-plane and out-of-plane $C\equiv C-H$ bends, are difficult to predict, being much too high at the HF level and much too low at the MP2 level. As already indicated, the MP2/6-31G(d) basis set is not sufficiently large to be a good predictor for triple bonds. In the case of such bonds, the mean of the HF and MP2 predictions appears to be close to or slightly higher than the observed frequency. The $\nu_{18}$ mode is also affected because of the large $S_{17}$ contribution for both the *trans* and *gauche* conformers. Calculation of vibrational frequencies with a larger basis set, MP2/6-311G(d), has been made for the *trans* conformer, and while the frequencies of these difficult modes have been raised by 20−30 $cm^{-1}$, they are not raised sufficiently to merit further tabulations.

## Torsional Transitions

As in 1,2-pentadiene, there are two torsional modes in 1-pentyne, the asymmetric skeletal torsion and the methyl internal rotation. According to the *ab initio* energy calculations, the methyl group shows a high barrier to internal rotation, and from the structure one might expect the barrier to methyl torsion to be of the same order as in ethane. From the *ab initio* calculation of harmonic force constants from the MP2/6-31G(d) calculation, the methyl torsional frequency given in Table 5 is 248 $cm^{-1}$ for the *trans* and 259 $cm^{-1}$ for the *gauche* conformers. On the basis of both *ab initio* frequency and intensity predictions, the series of Q peaks around 250 $cm^{-1}$ (Figure 7) are reasonably assigned to methyl torsional transitions of *gauche* 1-pentyne. Confirmation of this assignment is given by the rotational sub-band structure on the high-frequency side with a mean interval of 0.42 $cm^{-1}$, which does not correspond to the *trans* rotational constants. In fact, for a molecule with a planar skeleton which is nearly a symmetric top, the band contour for an out-of-plane (C-type) transition should not show strong central peaks. Methyl torsional transitions of the *trans* form may be absent in view of the very small calculated intensity (Table 5). However, the fact that the *gauche* conformer

dominates the far infrared spectrum does not mean that it is lower in energy, but it is probably due to its larger dipole derivatives (Table 5) for most modes whose transitions are seen in the far infrared spectrum.

The methyl torsional frequency may also be found from the barrier of the usual methyl torsional potential energy function. The *ab initio* energies of fully optimized staggered and eclipsed forms have been employed and are listed in Table 2 for both conformers. For most *ab initio* methods, the methyl barrier for the *gauche* form is slightly higher than that for the *trans* rotamer. The torsional kinetic constants *F* have been obtained from the MP2/6-31G(d) geometries and are given in Table 3. It is evident from the number of Q peaks and the intervals between them that they do not all fit one series of consecutive transitions. Choosing the most prominent series of three bands, a good fit is obtained using the *F* constant of *gauche* and varying both $V_3$ and $V_6$ constants. A further two series with three Q peaks each can also be fitted, and higher values of $V_3$ are obtained as they start with transitions at progressively higher frequencies. These transitions probably arise as hot bands involving one or more of the low-frequency modes, namely, skeletal bending $\nu_{20}$ and asymmetric torsion $\nu_{33}$.

Approximate values of the asymmetric torsion fundamentals of 114 and 106 $cm^{-1}$ for *gauche* and *trans* 1-pentyne, respectively, have been obtained from satellite line intensities in the microwave spectrum.[3] The *ab initio* predictions from harmonic force constants are very similar at 115 and 99 $cm^{-1}$ for *gauche* and *trans* conformers, respectively, but their predicted intensities are rather small. Very weak absorption can also be seen in Figure 1, with maxima at 114 and 109 $cm^{-1}$. There is also a very weak feature starting at 279 $cm^{-1}$ with rotational fine structure degrading to low frequencies which can be assigned to a combination of 114 and 168 $cm^{-1}$, and since 168 $cm^{-1}$ is firmly assigned to $\nu_{20}$ of the *gauche* conformer, the 114 $cm^{-1}$ peak is undoubtedly the asymmetric torsional fundamental of the *gauche* conformer.

## Discussion

Vibrational frequencies of both *gauche* and *trans* conformers of 1-pentyne were previously assigned in the mid-infrared spectrum, and it is now shown that vibrational bands of both conformers are also present in the far infrared spectrum in the gas phase at room temperature. The temperature study of the infrared spectrum of xenon solutions indicates that the *trans* conformer is the more stable rotamer in this solution. Since the dipole moments and molecular volumes of the two conformers are nearly the same, one expects that the stability in the xenon solution should be the same as that in the gas. However, the *ab initio* calculations with electron correlation with a relatively large basis set, i.e. MP2/6-311+G(d,p), predict the *gauche* conformer as the more stable form by 103 $cm^{-1}$ (295 cal/mol), which casts some doubt on the conformer that is the more stable form in the gas phase. A temperature study of the infrared spectrum of the gas would be of interest for resolving this difference. However, it should be noted that for the *n*-butane molecule the *trans* form is more stable by 234 ± 33 $cm^{-1}$ than the *gauche* form in the gas phase.[6] Thus, it would be surprising if the acetylenic group would alter the conformational stability by such a large amount that the *gauche* conformer is the more stable form in the gas phase. Additionally, it should be noted that butyronitrile, $CH_3CH_2CH_2CN$, which is isoelectronic to 1-pentyne has the *trans* conformer more stable than the *gauche* form.[13] It would be of interest to see if *ab initio* calculations at the level utilized in our study of 1-pentyne also predict the *gauche* conformer more stable for butyronitrile.

Infrared intensities were calculated on the basis of the dipole moment derivatives with respect to the Cartesian coordinates. The derivatives were taken from the *ab initio* calculations (MP2/6-31G[d]) and transformed to normal coordinates by

$$\left(\frac{\partial \mu_u}{\partial Q_i}\right) = \sum_j \left(\frac{\partial \mu_u}{\partial X_i}\right) L_{ji}$$

where the $Q_i$ is the *i*th normal coordinate, $X_j$ is the *j*th Cartesian displacement coordinate, and $L_{ji}$ is the transformation matrix between the Cartesian displacement coordinates and normal coordinates. The infrared intensities (MP2/6-31G[d]) were then calculated by

$$I_i = \frac{N\pi}{3c^2}\left[\left(\frac{\partial \mu_x}{\partial Q_i}\right)^2 + \left(\frac{\partial \mu_y}{\partial Q_i}\right)^2 + \left(\frac{\partial \mu_z}{\partial Q_i}\right)^2\right]$$

The predicted infrared spectra in the region 700−1500 $cm^{-1}$ of the *trans* and *gauche* conformers are shown in Figure 3D,C, respectively. The mixture of the two conformers with an assumed $\Delta H$ of 113 $cm^{-1}$ with the *trans* conformer the more stable rotamer is shown in Figure 3B. Since the calculated frequencies are approximately 10% higher than those observed, the frequency axis of the theoretical spectrum was shifted by a factor of 0.9. The calculated spectrum is in good agreement with the experimental spectrum of the sample dissolved in xenon (Figure 3A) except there are three *gauche* bands whose relative intensities are slightly higher in intensity than those predicted. Nevertheless, the predicted spectrum clearly shows the utility of the calculated infrared intensities for analytical purposes and for supporting vibrational assignments.

Raman spectra were also calculated (Figure 2) using frequencies and Raman scattering activities (MP2/6-31G[d]) determined from the *ab initio* calculations. The Raman scatter cross sections, $\partial\sigma_j/\partial\Omega$, which are proportional to the Raman intensities, can be calculated from the scattering activities and the predicted frequencies for each normal mode using the relationship[14]

$$\frac{\partial \sigma_j}{\partial \Omega} = \left(\frac{2^4\pi^4}{45}\right)\left(\frac{(\upsilon_0 - \upsilon_j)^4}{1 - \exp[-hc\nu_j/kT]}\right)\left(\frac{h}{8\pi^2 c\nu_j}\right)S_j$$

where $\nu_0$ is the exciting frequency, $\nu_j$ is the vibrational frequency of the *j*th normal mode, and $S_j$ is the corresponding Raman scattering activity. To obtain the polarized Raman scattering cross sections, the polarizabilities are incorporated into $S_j$ by $S_j[(1 - \rho_j/(1 + \rho_j)]$, where $\rho_j$ is the depolarization ration of the *j*th normal mode. The Raman scattering cross sections and calculated frequencies were used together with a Lorentzian line shape function to obtain the calculated spectrum. The predicted Raman spectra of the *trans* and *gauche* conformers are shown in Figure 2D,C, respectively. In Figure 2B, the mixture of the two conformers is shown, and in Figure 2A the experimental Raman spectrum of the liquid is presented. The predicted spectrum shows fair agreement with the experimental spectrum with the major differences in the carbon−hydrogen stretching region and the low-frequency region, where the lines appear to be much closer than those predicted. Also, the doublet in the 800 $cm^{-1}$ region has the line assigned to the *trans* conformer significantly more intense than the predicted value relative to the corresponding line assigned to the *gauche* conformer.

We have calculated the depolarization ratios for the fundamentals for both conformers (Table 5). These data are compared to the experimental values, and for most of the fundamentals

**TABLE 6: Potential Energy Functions and Torsional Transitions[a] for Methyl Torsions of 1-Pentyne in the *Gauche* and *Trans* Conformations**

| | *gauche* | | | |
|---|---|---|---|---|
| | obs. 1st series | fit[b] 1st series | fit[c] 2nd series | *trans* fit[c] 3rd series |
| F | | 5.4583 | 5.4583 | 5.4583 |
| $V_3$ | | 1534.5 | 1678.4 | 1730.9 |
| $V_6$ | | −44.3 | −85.1 | −97.0 |
| 1 ← 0 | 249.81 | 249.72 | 251.91 | 253.46 |
| 2 ← 1 | 239.25 | 239.98 | 245.25 | 247.58 |
| 3 ← 2 | 229.26 | 228.40 | 237.77 | 241.25 |

[a] All constants and transitions in $cm^{-1}$. Only the A−A transitions are shown and fitted, but the A−A/E−E splittings are very small for the transitions listed. [b] Fitted potential constants with calculated wavenumbers for comparison with observed. [c] Observed wavenumbers with fitted potential constants.

the agreement is reasonably good, particularly when one considers that most of the lines have contributions from both conformers.

The $V_n$ constants for the potential function for asymmetric torsion

$$V(\tau) = \sum_n {}^1/_2 V_n(1 - \cos n\tau)$$

have been derived from the microwave spectrum by a fitting technique[3] and are given in Table 7. The signs of the $V_n$'s correspond to $\tau = 0°$ at the *trans* position, and hence the *gauche* minimum is at 115°. Since the torsional energy levels were not previously calculated[3] using a series of $F$ constants from a flexible structural model, the two torsional fundamentals of 114 and 109 $cm^{-1}$ (106 $cm^{-1}$ from microwave study) have been refitted by adjusting the potential constants utilizing the *gauche* dihedral angle of 114.6° (61.6°). However, these determined potential parameters are not significantly different from those reported[3] earlier.

From the *ab initio* energies given in Table 2, a four-term potential function was determined, and this calculation yields the values of the torsional fundamentals of 122.7 and 107.5 $cm^{-1}$, in reasonable agreement with the observed values. However, a value of $V_4$ of opposite sign of that predicted from the microwave data is obtained. On fitting the two frequencies (microwave values) for the torsional fundamentals by adjusting $V_3$ and $V_4$, a function very similar to that from the microwave data is obtained except for the larger conformational energy difference of −45.5 $cm^{-1}$. The agreement between the microwave and *ab initio* potential energy functions is good except for the torsional angle of the *gauche* conformer.

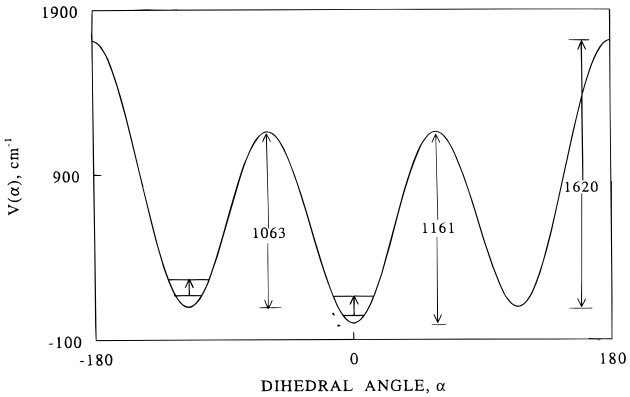


**Figure 8.** Potential function of the asymmetric torsional motion of 1-pentyne. The dihedral angle of 0° corresponds to the *trans* conformer (note: the dihedral angle of the *gauche* conformer is 360° minus the angle listed in Table 3).

We have also determined the potential parameters utilizing the $\Delta H$ value obtained from the xenon solution, the torsional frequencies from both the far infrared and microwave data, and the *gauche* dihedral angels from the *ab initio* predicted value and the microwave results (Figure 8). With the smaller *gauche* dihedral angle (Table 7, column 5) the $V_2$ term is similar to that obtained from microwave data, but the $V_1$ term is significantly larger because of the larger positive value of the $\Delta H$ (*trans* more stable) compared to the −25.4 $cm^{-1}$ (*gauche* more stable) value for $\Delta H$ from the microwave results. As the *gauche* dihedral angle approaches the value of 120°, which is the value for a pure 3-fold rotor, the $V_2$ and $V_4$ values are nearly zero and the value of the $V_1$ term is reduced significantly. The actual value is probably between these two extremes since it is doubtful that the *gauche* dihedral angle is as large as 119.4°, but it is probably not as small as 115.0° either. Changes in the $\Delta H$ value with the listed experimental uncertainties would significantly change only the value of the $V_1$ term. Therefore, to obtain more accurate values of the potential parameters governing the conformational interchange requires a more definitive determination of the *gauche* dihedral angle, possibly from an electron diffraction study of 1-pentyne.

**TABLE 7: Potential Energy Functions and Torsional Transitions[a] in ($cm^{-1}$) for Asymmetric Torsions of 1-Pentyne from Microwave Spectroscopy and *ab Initio* Calculations and Fits to Microwave Data**

| | MW[b] | MW adjusted and fitted | *ab initio*[c] four-term PEF | *ab initio* adjusted and fitted | exptl fit 1[d] | exptl fit 2[e] |
|---|---|---|---|---|---|---|
| $V_1$ | 328.8 | 328.8 | 187.8 | 190.4 | 450.5 | 132.7 |
| $V_2$ | −365.5 | −365.5 | −249.2 | −279.3 | −315.2 | 8.8 |
| $V_3$ | 1230.4 | 1258.8 | 1397.1 | 1251.8 | 1267.2 | 1253.8 |
| $V_4$ | 24.8 | 50.0 | −32.3 | 41.0 | 23.5 | 5.0 |
| t/g[f] | 1061.6 | 1110.2 | 1233.0 | 1125.3 | 1161.1 | 1297.6 |
| g/g[f] | 1590.0 | 1602.9 | 1659.4 | 1491.7 | 1620.0 | 1276.9 |
| $\Delta E_{\text{gauche−trans}}$ | −30.8 | −15.7 | −74.6 | −49.6 | 97.8 | 109.6 |
| $\tau_{\text{min}}$ | 115.0 | 114.6 | 117.2 | 116.1 | 115.0 | 119.4 |
| $1^{\pm} \leftarrow 0^{\mp}$ | 114.0 | 114.0 | 122.7 | 113.9 | 114.0 | 113.4 |
| $2^{\pm} \leftarrow 1^{\mp}$ | | | 120.0 | 111.4 | 111.3 | 110.6 |
| 1 ← 0 | 106.0 | 106.0 | 107.5 | 106.0 | 106.0 | 109.0 |
| 2 ← 1 | | | 104.9 | 103.2 | 103.2 | 106.4 |
| $\Delta H_{\text{gauche−trans}}$ | −25.4 | −11.6 | −66.8 | −45.5 | +103.2 | +112.1 |

[a] Calculated transition wavenumbers obtained using a series of $F$ kinetic constants calculated from the MP2/6-31G(d) geometric structures of both *trans* and *gauche* conformers. Part of the cosine series is $F_0 = 1.2130$, $F_1 = -0.2644$, $F_2 = 0.1636$, $F_3 = -0.0502$, $F_4 = 0.0196$, $F_5 = -0.0069$ $cm^{-1}$. [b] Reference 3. [c] Potential constants from MP2/DZ(d) energies. [d] To torsional transitions 114 and 109 $cm^{-1}$, $\Delta H = 113$ $cm^{-1}$, and $t_{\text{min}} = 115.0$. [e] To torsional transitions 114 and 109 $cm^{-1}$, $\Delta H = 113$ $cm^{-1}$, and $t_{\text{min}} = 119.4$. [f] *Trans/gauche* and *gauche/gauche* energy barriers.

**Acknowledgment.** J.R.D. would like to acknowledge partial support of these studies by the University of Missouri—Kansas City Faculty Research Grant program.

## References and Notes

(1) Bell, S.; Guirgis, G. A.; Durig, J. R. *Spectrochim. Acta* **1996**, *52A*, 1843.

(2) Damiani, D.; Mirri, A. M. *Chem. Phys. Lett.* **1971**, *10*, 351.

(3) Wodarczyk, F. J.; Wilson, E. B. *J. Chem. Phys.* **1972**, *56*, 166.

(4) Crowder, G. A.; Fick, H. *J. Mol. Struct.* **1986**, *147*, 17.

(5) Crowder, G. A. *J. Mol. Struct.* **1988**, *172*, 151.

(6) Herrebout, W. A.; van der Veken, B. J.; Wang, A.; Durig, J. R. *J. Phys. Chem.* **1995**, *99*, 578.

(7) Furic, K.; Durig, J. R. *Appl. Spectrosc.* **1988**, *42*, 175.

(8) Frisch, M. J.; Trucks, G. W.; Schlegel, H. B.; Gill, P. M. W.; Johnson, B. G.; Robb, M. A.; Cheeseman, J. R.; Keith, T. A.; Petersson, G. A.; Montgomery, J. A.; Raghavachari, K.; Al-Laham, M. A.; Zakrzewski, V. G.; Ortiz, J. V.; Foresman, J. B.; Cioslowski, J.; Stefanov, B. B.; Nanayakkara, A.; Challacombe, M.; Peng, C. Y.; Ayala, P. Y.; Chen, W.; Wong, M. W.; Andres, J. L.; Replogle, E. S.; Gomperts, R.; Martin, R. L.; Fox, D. J.; Binkley, J. S.; Defrees, D. J.; Baker, J.; Stewart, J. P.; Head-Gordon, M.; Gonzalez, C.; Pople, J. A. *Gaussian 94 (Revision B. 3)*; Gaussian Inc.: Pittsburgh, PA, 1995.

(9) Moller, C.; Plesset, M. S. *Phys. Rev.* **1934**, *46*, 618.

(10) Durig, J. R.; Guirgis, G. A.; Bell, S.; Brewer, W. E. Submitted to *J. Phys. Chem.*

(11) Durig, J. R.; Guirgis, G. A.; Bell, S. To be published.

(12) Schachtschneider, J. H. Vibrational Analysis of Polyatomic Molecules, Parts V, VI. Tech. Rep. Nos. 231 and 57; Shell Development Co.: Houston, TX, 1964 and 1965.

(13) Wlodarczak, G.; Martinache, L.; Demaison, J.; Marstokk K. M.; Mollendal, H. *J. Mol. Spectrosc.* **1988**, *127*, 178.

(14) Chantry, G. W. In *The Raman Effect*; Anderson, A., Ed.; Marcel Dekker: New York, 1991; Vol. 1.